Supplementary Information (SI) for Journal of Materials Chemistry C.

Supplementary Information

Conductive/Non-Conductive Bi-compartmental Architectures for Sensing Applications

Yafei Yang,[a] Zhe Ma,[a] Jingxin Gao,[b] Ruotong Liu,[a] Aierpati Abudusaimaiti,[a] and Jiguang Liu*[a]

[a] School of Materials Design & Engineering, Beijing Institute of Fashion Technology, Beijing 100029, P. R. China

[b] College of Arts and Sciences, Beijing Institute of Fashion Technology, Beijing 100029, P.R. China

*Email: J.liu@bift.edu.cn

1. Experimental Section

1.1 Preparation of bi-compartmental particles

A home-made microfluidic device was fabricated using silicone tubing and a microinjector. Polyaniline was incorporated into polyethylene glycol diacrylate (PEGDA) containing a photoinitiator to form a conductive miscible solution, where polyaniline acted as the conducting material and the photopolymerizable monomer PEGDA served as the matrix. Another solution was prepared with acrylic acid (AA), *N*-isopropylacrylamide (NIPAM) and photoinitiator, in which AA is used as the hydrophilic functional group and grafting site, while NIPAM acts as the carrier for the thermoresponsive component. The two solutions were respectively used as two dispersion phases for creating particles under UV light with 365 nm wavelength, while dimethylsilicone oil was used as the continuous phase. By adjusting the flow rate ratio of two dispersion phase, a series of bi-compartmental particles with different volume ratios of the two components were prepared. A typical preparation is described as below:

0.28 g of polyaniline and 0.1 g of photoinitiator A89077 (2-hydroxy-4'-(2-hydroxyethoxy)-2-methylpropiophenone) are dispersed in 2 g of PEGDA solution with a concentration of 1.1g/mL, which was used a dispersion phase, i.e., EG-AN phase.

1 g of NIPAM (1g), 0.08g of BIS, 0.1 g of acrylic acid (AA), and 0.05 g A89077 are dissolved in 3.5 mL deionized water, while 0.5 mL of ethanol is added as a cosolvent, which is used as the second dispersion phase, named as NI-AA phase.

Dimethyl silicone oil is used as the continuous phase. The total flow rate of the two dispersed phases is 0.1 ml/h. The size of the two components in particles is controlled by adjusting the flow rate ratio of the two dispersion phases. The samples are named with their flow velocity ratio of EG-AN (i.e., V_{EG-AN}), for example, the flow velocity ratio of EG-AN phase to NI-AA phase is 0.02 ml·h^{-1}/0.08 ml·h^{-1}, referred to E2. When the asymmetric particles flow out from the channel, they are collected after washed three times with toluene and anhydrous ethanol. The obtained particles are stored at room temperature.

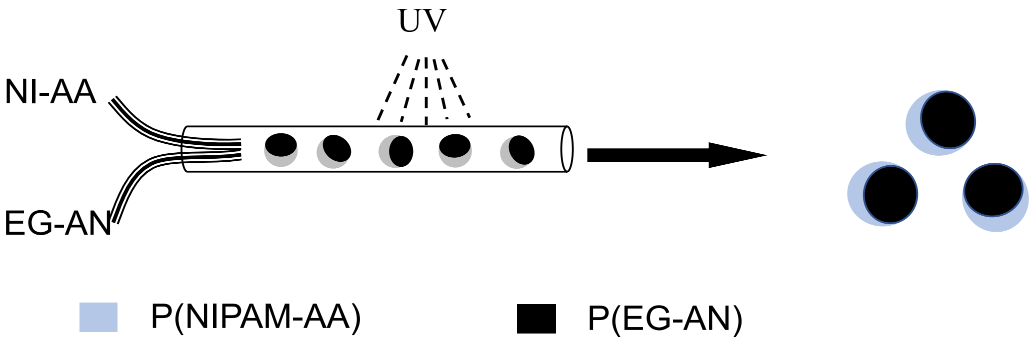

Scheme S1. Schematic illustration of preparing conductive/non-conductive bi-compartmental particles with microfluidic technology.

1.2 Preparation of bilateral fibers

Similarly, bi-compartmental bilateral fibers could be fabricated with the microfluidic equipment. We used polyurethane in *N,N*-dimethylacetamide (DMAC) solution with a concentration of 40 wt% as polymer phase, i.e., PU phase, and use polyaniline particles dispersed in polyurethane solution with a certain concentration as conductive phase. After the bi-compartmental solution flow out of the channel, it enters an aqueous solution for getting a bilateral fiber. The bilateral fibers were then washed enough with ethanol and water.

1.3 Characterization

The morphologies of particles and fibers were characterized with microscopes (BX 41, Olympus Corp., Japan). Their morphologies were also checked with scanning electron microscopy (JSM-7500F JEOL environmental scanning electron microscope, Japan Electronics Co., Ltd.) at a voltage of 5 kV and a current of 10 μA. Before characterization with SEM, the samples were directly put onto a carbon adhesive and then sputtered with platinum. The surface compositions of particles were characterized by Fourier transform infrared (FTIR) spectroscopy measurements with a Bruker TENSOR 27 FTIR spectrometer.

The electric resistances were measured with an Avometer (17B Digital Multimeter, Fluke Cooperation) under pressure with a Push Tension Tester, which is illustrated as Figure S2. The testing setup mainly consisted of a lifting platform, ITO glass, an insulating gasket, and a push tension tester. In the setup, the ITO glass was fixed between the lower surface of the push-pull rod of push-tension testing machine and the upper surface of the lifting platform, serving as the two electrode plates. The insulating gasket, with a hole of 0.5 cm in length at the center and a thickness smaller than 25 μm, was covered on the conducting ITO glass of the lifting platform to prevent short circuit caused by the contact between the upper and lower ITO glasses in measuring the resistance of the particles. During the test, a certain amount of bi-compartmental conductive particles was placed in the center hole of the insulating gasket, and the rotating wheel on the push-pull rod of the tensile testing machine was shaken to make the conducting glasses approach each other. Once the upper and lower conducting glasses touch the particles, the applied pressure can be adjusted.

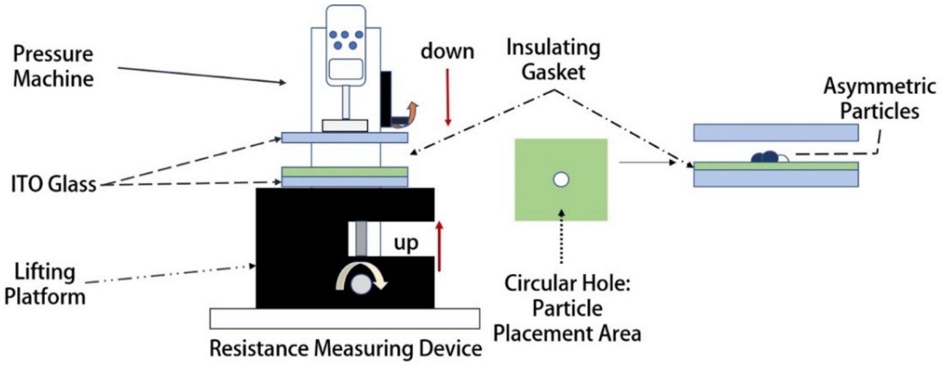

Scheme S2. Schematic diagram of the device for measuring the resistance of bi-compartmental particles.

The Sensing devices were designed according to Scheme 3, and the additional performances were further shown in Figure S11-15, Supporting Video 1-3. All human subjects involved in this research have provided informed consent for their participation and for the publication of their images.

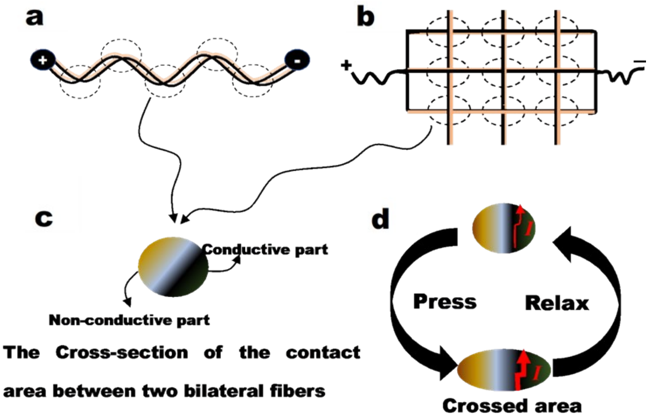

Scheme S3. Schematic illustration of measuring the sensing property of the two modes of weaving bilateral fibres. a) the twisted two fibres; b) the weaving fibres; c) the cross-section of the crossed sites between two fibres (the circle sites in a and b); d) The change of the crossed sites under pressure, resulting in the change of conductive areas.

2. Supporting Figures

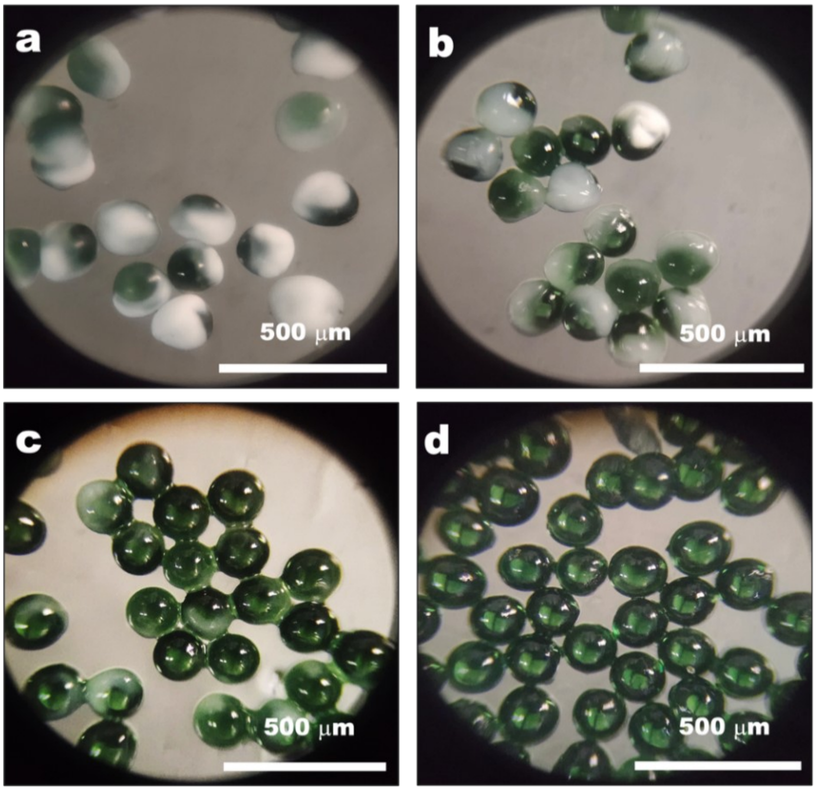

Figure S1. Microscopic images of P (NIPAM-AA)/P(EG-AN) bi-compartmental particles with different flow velocity ratio EG-AN phase to NI-AA phase. a) 2:8; b) 3:7; c) 4:6; d) 5:5, respectively named as E2, E3, E4 and E5.

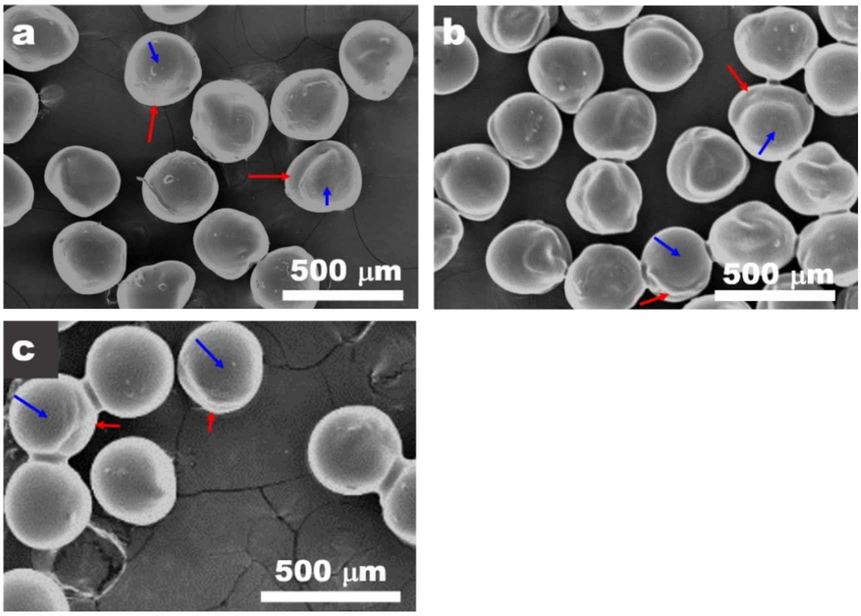

Figure S2. SEM images of P(NIPAM-AA)/P(EG-AN) bi-compartmental particles with different flow ratio EG-AN phase to NI-AA phase (the red arrow represents P(NIPAM-AA) part, and the blue arrow represents P(EG-AN) part. a) E2; b) E3; c) E5.

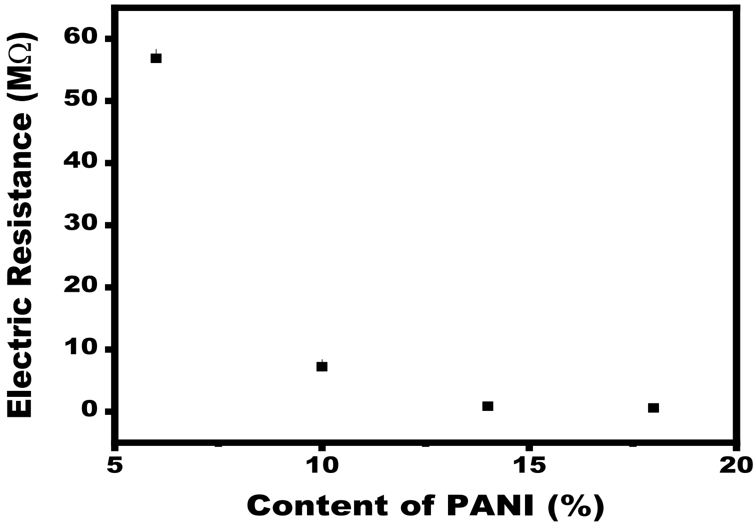

Figure S3. Electric resistance of bi-compartmental particles dependent on the feed ratio of PANI.

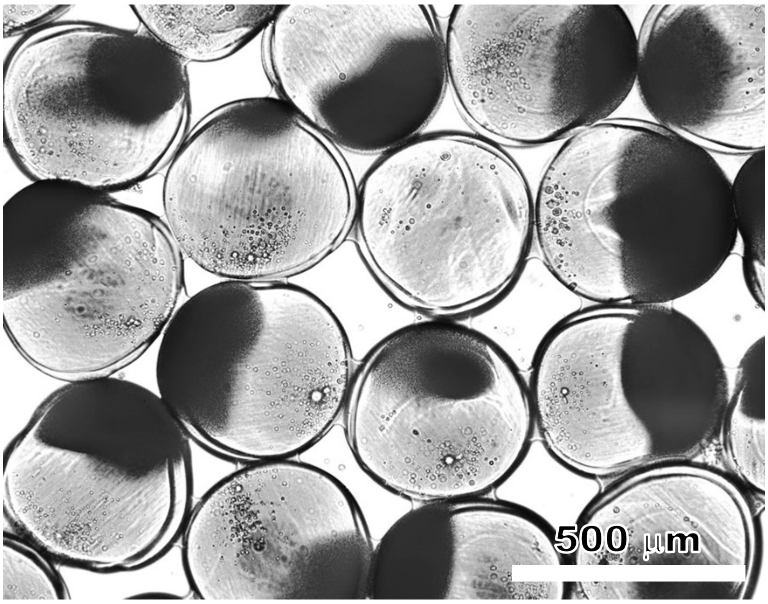

Figure S4. Microscopic photos of wet bi-compartmental particles.

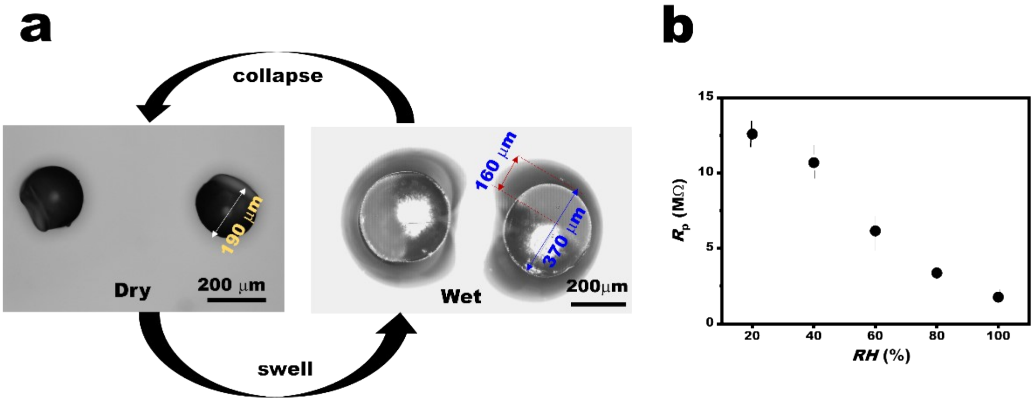

Figure S5. The resistance of bi-compartmental particles dependent on circumstance. a) the morphology of bi-compartmental particles (E3) responsive to humidity; b) the electric resistance of bi-compartmental particles responsiveness to humidity. The photos were taken with microscopy in polarized mode.

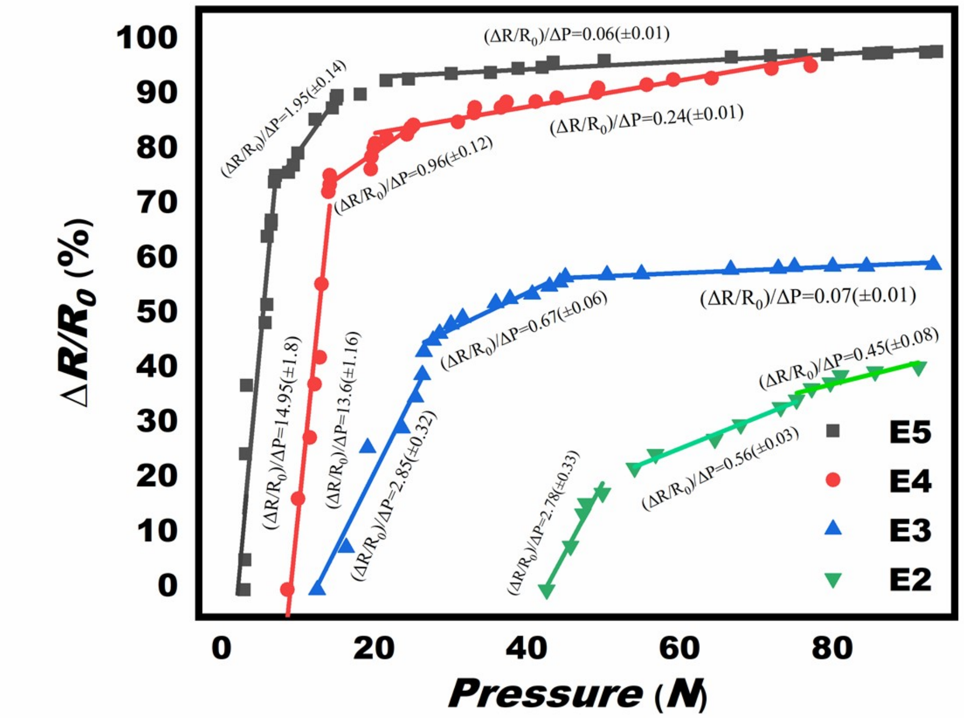

Figure S6. Relative resistance variation of bi-compartmental particles with different ratios of conductive compartments dependent on pressure with the fitted sensitivities.

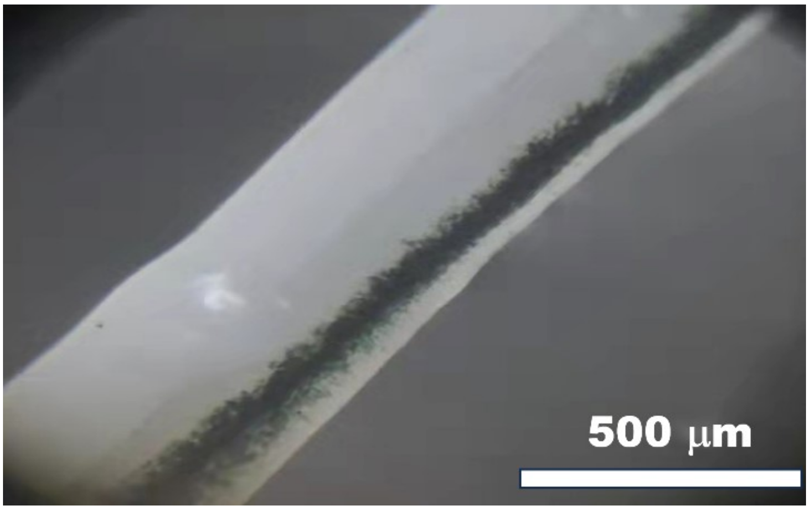

Figure S7. The images of a P(EG-AN)/P(NI-AA) bilateral fiber.

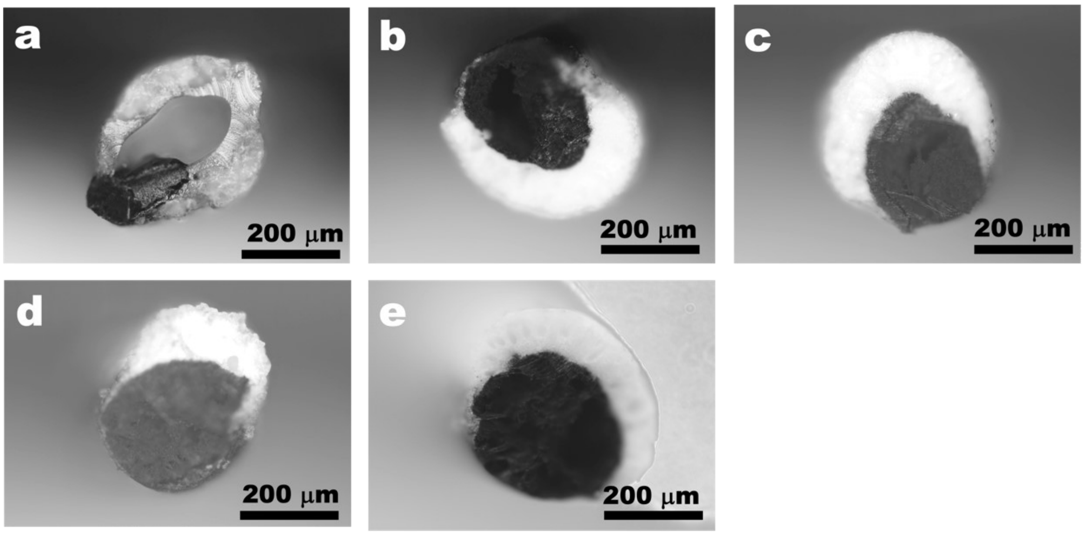

Figure S8. Microscopic photos of PAU/PU bilateral fibers with different ratios of V_{AU}. a) 3:7; b) 4:6; c) 5:5; d) 6:4; e) 7:3.

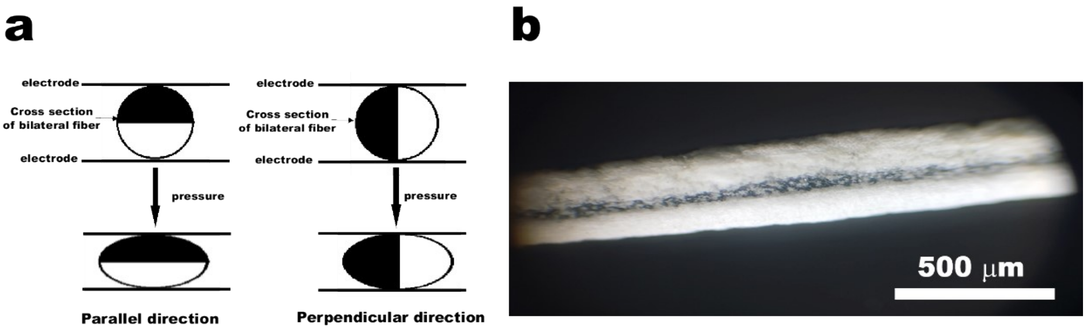

Figure S9. The shape change of bilateral fiber under pressure. a) a schematic illustrated direction of a fiber cross section between two electrodes; b) a photo of bilateral fiber after the fiber with a parallel direction was pressed.

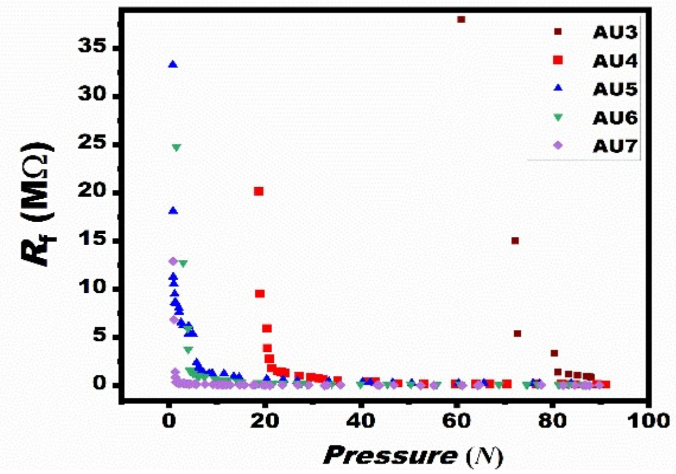

Figure S10. Electric resistance of bilateral fibers with different ratios of V_{AU} under pressure.

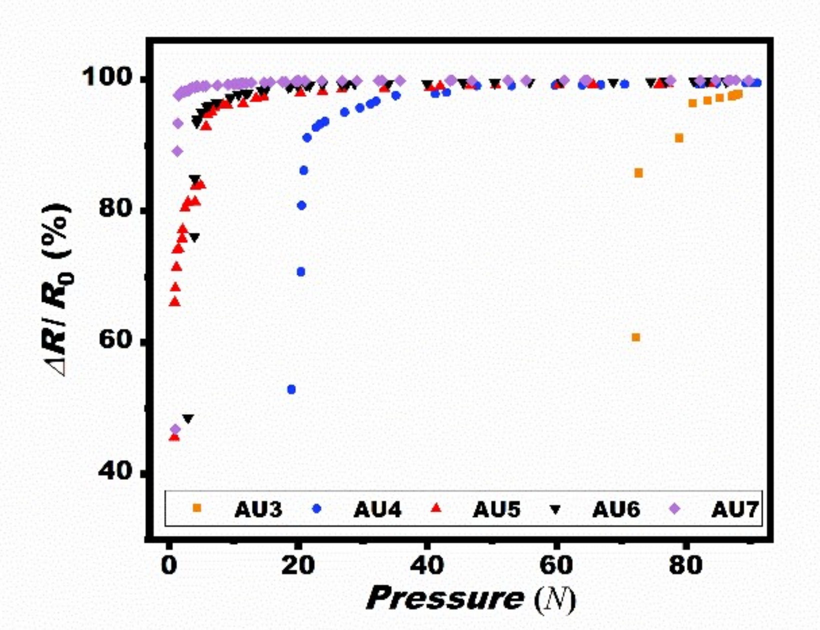

Figure S11. The relative resistance variation of bilateral fibers with the different V_{AU} ratios dependent on pressure.

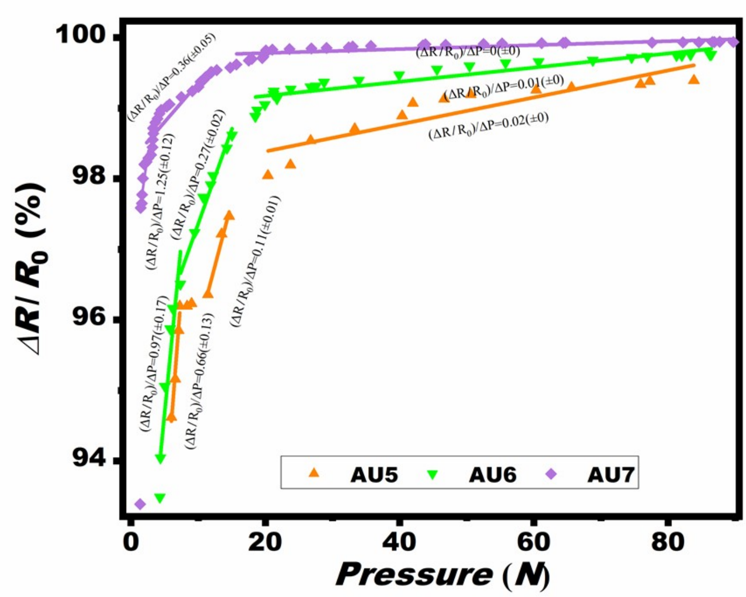

Figure S12. The curves of relative resistance variation of bilateral fibers versus pressure with the linear fitting.

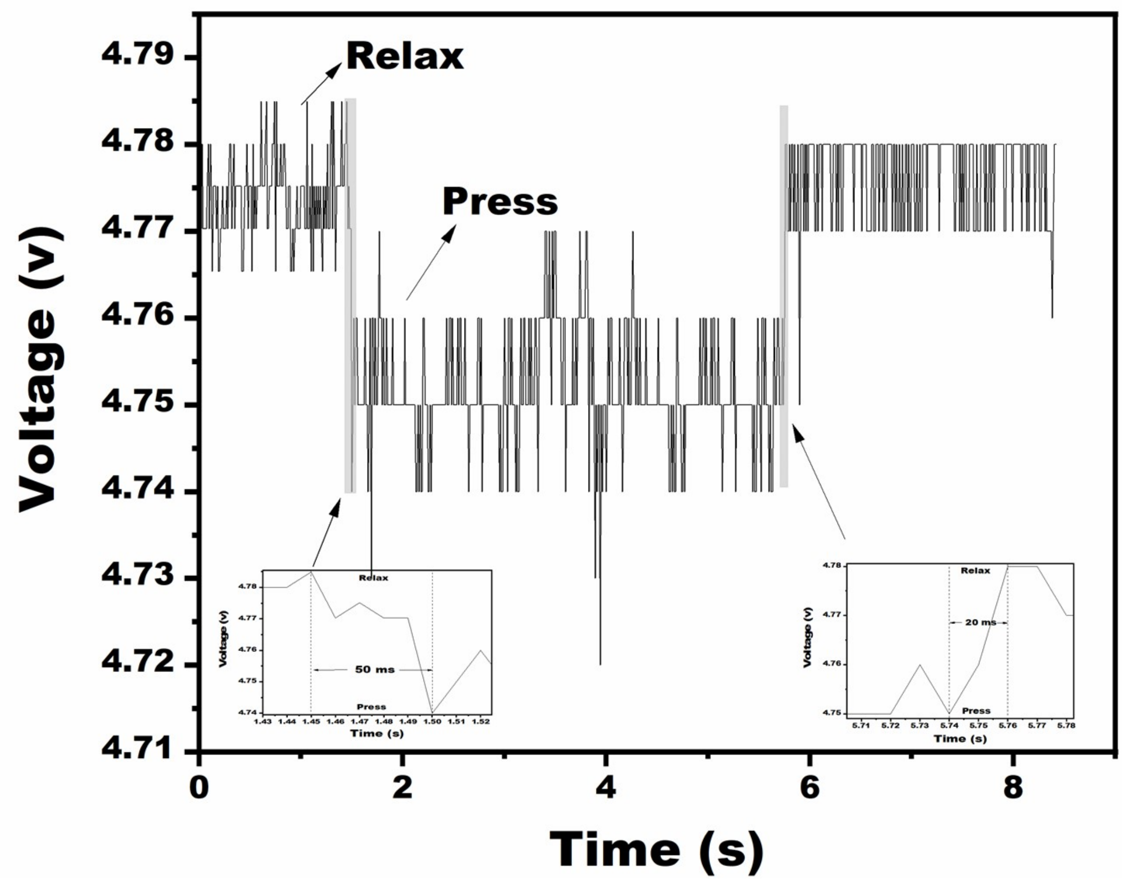

Figure S13. The response time of twisted fibres.

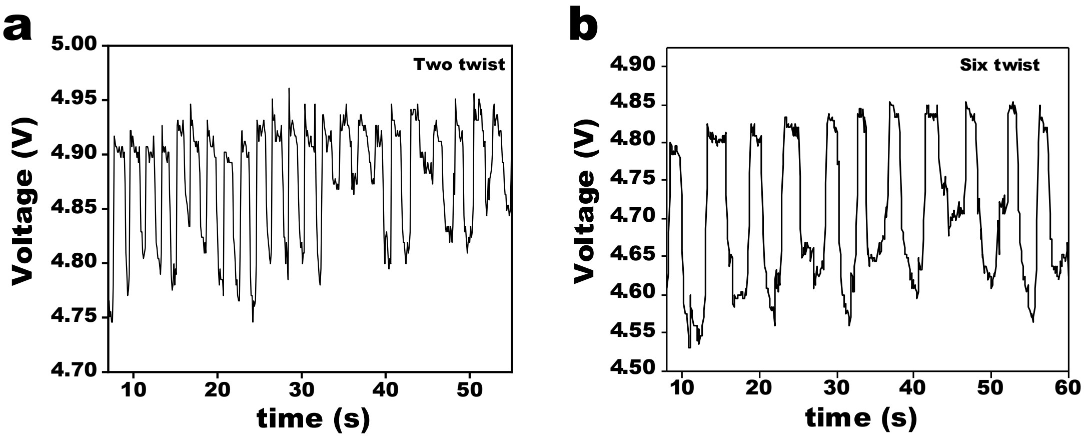

Figure S14. The output voltage of twisted fibres under pressure. a) two twists; b) six twists.

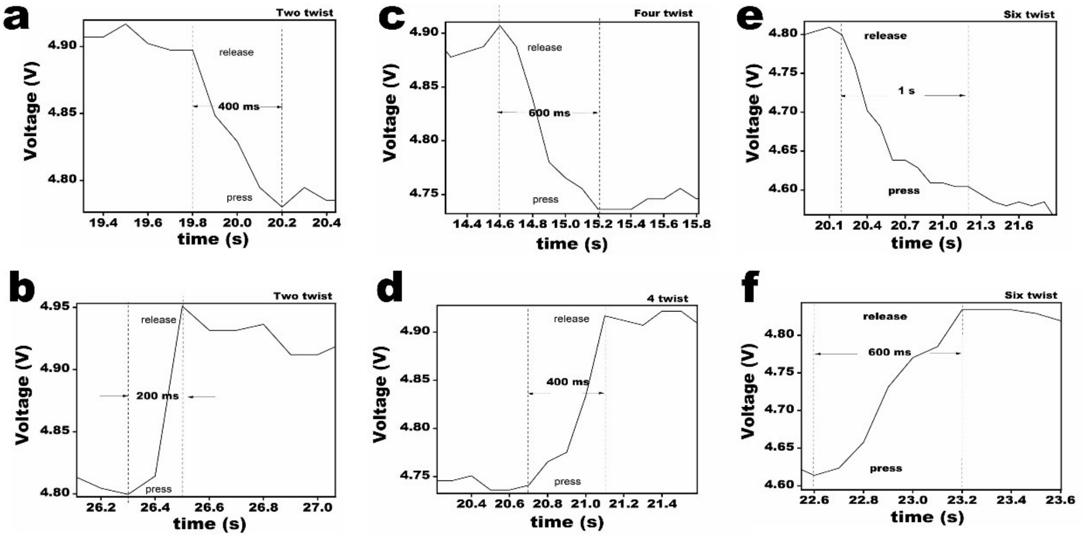

Figure S15. Response time of the fibres with different twist numbers under pressure.

Figure S16. A photo of a woven grid with bilateral fibres on a finger (the black is the insulating tape)

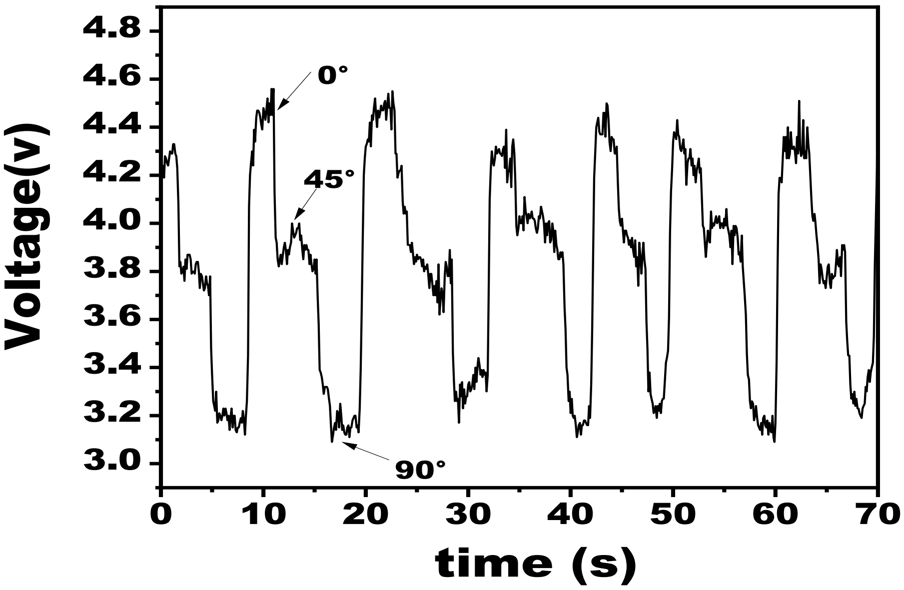

Figure S17. A repeated outputted voltage of a woven grid on fingers accompany with its bending.

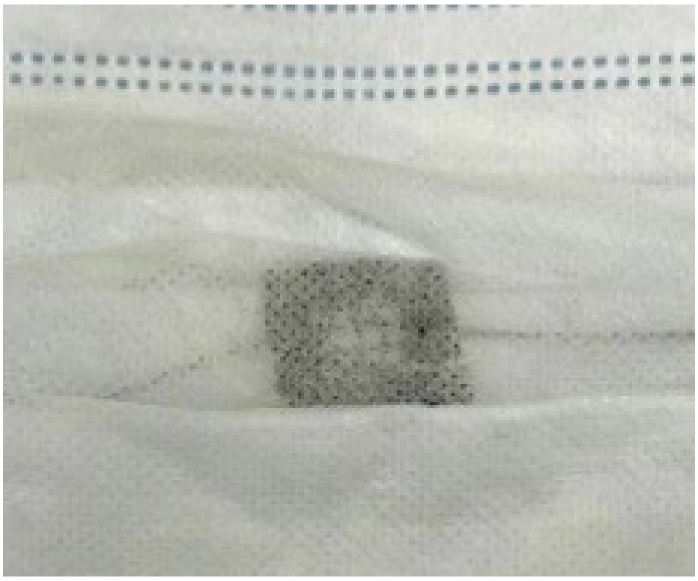

Figure S18. A photo of a woven grid with bilateral fibres inside a mask.

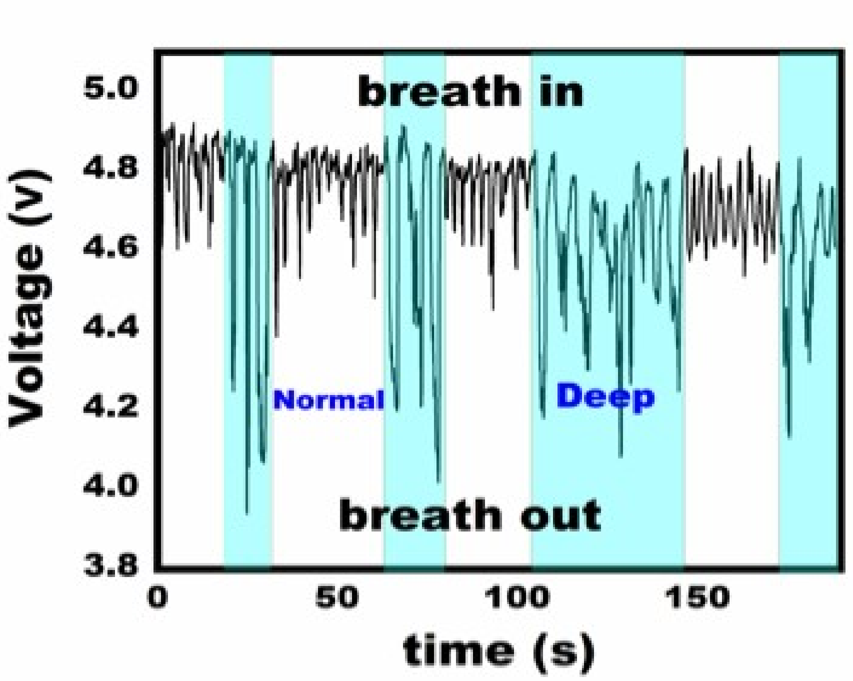

Figure S19. A repeated outputted voltage of a woven grid with bilateral fibres inside a mask during human breath.